

RLIP76 Transports Vinorelbine and Mediates Drug Resistance in Non–Small Cell Lung Cancer

David Stuckler,¹ Jyotsana Singhal,¹ Sharad S. Singhal,¹ Sushma Yadav,¹ Yogesh C. Awasthi,² and Sanjay Awasthi¹

¹Department of Chemistry and Biochemistry, University of Texas at Arlington, Arlington, Texas and ²Department of Human Biological Chemistry and Genetics, University of Texas Medical Branch at Galveston, Galveston, Texas

Abstract

Vinorelbine (Navelbine), an amphiphilic semisynthetic *Vinca* alkaloid, has displayed superior activity and decreased resistance in the treatment of advanced non–small cell lung cancer (NSCLC) compared with other members of its class. Recently, vinorelbine and cisplatin combination chemotherapy has been shown for the first time to confer a significant survival advantage in early-stage lung cancer after surgical therapy. The biological mechanisms underlying the differential response of NSCLC to cytotoxic activity of vinorelbine have yet to be elucidated. Our recent findings indicate a role of RLIP76, a non-ATP binding cassette transport protein, in catalyzing the ATP-dependent efflux of structurally and functionally unrelated chemotherapeutic agents such as doxorubicin and vinblastine in NSCLC. Present studies were conducted to assess whether RLIP76 mediates vinorelbine transport and resistance. Here we show that RLIP76 catalyzes the transport of vinorelbine in a saturable manner with respect to vinorelbine (K_m 75 nmol/L) and ATP (K_m = 3.4 mmol/L). Three-fold overexpression of RLIP76 in NSCLC and SCLC confers increased resistance to cytotoxicity. RLIP76 overexpression causes a sustained intracellular decrease in vinorelbine concentration because of increased efflux, and anti-RLIP76 antibodies sensitize lung cancer cells to vinorelbine by inhibiting its efflux. These studies for the first time show that RLIP76 mediates vinorelbine transport and is capable of conferring drug accumulation defect and resistance to lung cancer cells. (Cancer Res 2005; 65(3): 991-8)

Introduction

Inherent drug resistance of non–small cell lung cancer (NSCLC) has significantly hampered attempts at curative. Previous attempts at adjuvant therapy of NSCLC have met with failure to improve survival, largely due to older and relatively ineffective chemotherapy agents (1–5). Vinorelbine, a relatively new semisynthetic *Vinca* alkaloid with significant activity in NSCLC and a relatively low toxicity profile even in the elderly (6–8), has recently been shown for the first time to prolong survival in early-stage NSCLC when given after successful resection in combination with cisplatin (9, 10). These findings have led to the adoption of vinorelbine-cisplatin chemotherapy as the first standard for adjuvant therapy of resected early-stage NSCLC.

Vinorelbine is a novel semisynthetic *Vinca* alkaloid, which differs from its predecessors in that it has a substitution on the catharanthine rather than the vindoline moiety of the molecule, which imparts increased lipophilicity, presumably allowing it to more readily diffuse into the cell. This modification probably accounts for the higher therapeutic index and different spectrum of antitumor activity (7, 11–14). In light of recent clinical findings of definite clinical benefit in NSCLC and because of the expected increase in the utilization of vinorelbine in NSCLC, elucidation of mechanisms used by cells to resist vinorelbine cytotoxicity may be of significant importance for optimizing lung cancer chemotherapy.

Although the molecular determinants of vinorelbine resistance are multiple, it is expected that multidrug resistance predominates (14). The expression of MDR1 gene product, Pgp, and MRP-1 are correlated with multidrug resistance associated with vinorelbine (14–16), and *Vinca* alkaloids are good substrates for these transporters (17, 18). Nonetheless, the existence of these pumps has not been able to adequately explain all types of vinorelbine resistance. Carcinoma cell lines expressing the vinorelbine-resistant phenotype have been reported that did not express Pgp (19). The level of MRP1 expression in tumor samples seems lower than surrounding tissue, and transport function does not correlate with MRP-1 expression (20). Furthermore, unlike vincristine, MRP-1 overexpression is not implicated in vinorelbine resistance (21). Therefore, the importance of transport mechanisms other than these ATP binding cassette (ABC) transporters cannot be ruled out (22, 23).

We have recently shown that RLIP76 (RALBP1), a non-ABC transporter, catalyzes energy-dependent efflux of a wide range of nonconjugated (unmodified) chemotherapeutics, including the *Vinca* alkaloids (24–29), as well as of glutathione conjugates of electrophilic compounds, including endogenous as well as exogenous alkylating agents. We have recently shown that RLIP76 represents the dominant mechanism for protection of cells from proapoptotic activities of alkylating lipid metabolites including 4-hydroxynonenal which are generated in response to stressors including UV light, heat, and oxidants (30, 31). RLIP76 is expressed strongly in lung cancer cells, functions to protect these cells from alkylating agent, *Vinca* alkaloid, and anthracyclines, and is significantly more active in NSCLC as compared with SCLC (25, 26). These findings suggested that RLIP76 plays a significant role in the inherent drug resistance of NSCLC. Since RLIP76 can transport *Vinca* alkaloids, including vincristine (26), vinblastine (24), and colchicine (32), we reasoned that it may also function as a vinorelbine transporter, and that the relatively greater cytotoxicity of vinorelbine could indicate that it is a relatively poor substrate for RLIP76. To validate this assertion, we did studies to assess the contribution of RLIP76 transport function towards the ATP-dependent vinorelbine efflux in lung cancer cells and its relevance to vinorelbine cytotoxicity.

Note: D. Stuckler and J. Singhal contributed equally to this communication.

Requests for reprints: Sanjay Awasthi, Department of Chemistry and Biochemistry, 502, Yates Street, Science Hall Room # 223, University of Texas at Arlington, Arlington, TX 76019-0065. Phone: 817-272-5444; Fax: 817-272-3808; E-mail: sawasthi@uta.edu.

©2005 American Association for Cancer Research.

Materials and Methods

Reagents. Cell culture reagents were obtained from Life Technologies Inc., Grand Island, NY. Chemical reagents and horseradish peroxidase-coupled goat anti-rabbit antibodies were purchased from Sigma Chemical Co., St. Louis, MO. DE-52 (DEAE cellulose) anion exchanger was purchased from Whatman International Ltd., Maidstone, England. Bio-Beads (SM-2 adsorbent) and Chelex-100 resin were purchased from Bio-Rad Laboratories (Hercules, CA). Tryptone and yeast extract for preparing culture media were purchased from Difco laboratories, Detroit, MI. Reagents for SDS-PAGE were purchased from Bio-Rad Laboratories. Vinorelbine (Navelbine) and doxorubicin (Adriamycin) were obtained from GensiaSicor Pharmaceutical (Irvine, CA) and Adria Laboratories (Columbus, OH), respectively. [³H]-Vinorelbine (specific activity, 7.5 Ci/mmol) and [¹⁴C]-doxorubicin (specific activity, 57 mCi/mmol) were purchased from ViTrax (Placentia, CA) and Amersham Co. (Arlington Heights, IL), respectively. Source of polyclonal rabbit anti-human rec-RLIP76 antibodies and protocol for purification of IgG were the same as previously described (28, 29). FITC-conjugated goat anti-rabbit antibodies were purchased from Vector Laboratories, Inc., Burlingame, CA. Ninety-six-well nitrocellulose membrane plates (pore size, 0.45 μm) used in transport studies were purchased from the Millipore Co. (Bedford, MA).

Cell Lines and Cultures. Human SCLC lines H1618 and NSCLC lines H1395, H2347, (adenocarcinoma), H520, H226 (squamous cell carcinoma), H358 (Bronchio alveolar), and H2126 (undifferentiated) were purchased from American Type Culture Collection, Manassas, VA. All cells were cultured at 37°C in a humidified atmosphere of 5% CO₂ in RPMI 1640 supplemented with 10% (v/v) heat-inactivated FBS, 1% (v/v) P/S solution, 2 mmol/L L-glutamine, 10 mmol/L HEPES, 1 mmol/L sodium pyruvate, 4.5 g/L glucose, and 1.5 g/L sodium bicarbonate.

Drug Sensitivity Assay. Cell density measurements were done using a hemocytometer to count reproductive cells resistant to staining with trypan blue. Approximately 20,000 cells were seeded into each well of 96-well flat-bottomed microtiter plates containing 160 μL RPMI. Post 24-hour incubation, 40 μL aliquots of drug (vinorelbine or doxorubicin) concentrations ranging from 1 to 10,000 nM were then added to eight replicate wells to assess the IC₅₀ of drug, defined as the concentration at which formazan was reduced by 50%. After either, 12, 24, or 96 hours of incubation, 20 μL of 5 mg/mL 3-(4,5-dimethylthiazol-2-yl)-2,5-diphenyltetrazolium bromide was introduced to each well and incubated for 2 hours of exposure. The plates were centrifuged and medium was decanted. Cells were subsequently dissolved in 100 μL DMSO with gentle shaking for 2 hours at room temperature, followed by measurement of absorbance at 570 nm (33).

Prokaryotic Expression of RLIP76. The 1,968-bp full-length open reading frame cDNA of human RLIP76 was cloned from a λgt11 human bone marrow library by immuno-screening using anti-DNP-SG ATPase antibodies and subcloned into the prokaryotic expression plasmid, pET-30a(+) (Novagen), creating the pET30-RLIP76 plasmid free of extraneous sequences. This plasmid was transformed into *Escherichia coli* BL21 (DE3). RLIP76 was expressed in *E. coli* BL21 (DE3) grown at 37°C after induction with 0.4 mmol/L isopropyl-L-thio-β-D-galactopyranoside (28).

Synthesis of S-(Dinitrophenyl) Glutathione. S-(Dinitrophenyl) glutathione (DNP-SG) was synthesized from CDNB and glutathione according to the method described by us previously (34). Recombinant hGSTA2-2 (35) was used to catalyze the conjugation of glutathione to CDNB.

Purification of Recombinant RLIP76. We have shown that a DNP-SG affinity resin prepared as previously described by us can be used to purify RLIP76 to near homogeneity (28). Amino acid analysis of the purified RLIP76 obtained by DNP-SG affinity chromatography showed composition within 96% of that expected for full-length RLIP76. Protein was estimated by the method of Minamide and Bamberg (36). Western blot analysis was done by the method of Towbin et al. (37), and PAGE was done in the system described by Laemmli (38).

Reconstitution of Purified RLIP76 into Artificial Liposomes. Reconstitution of rec-RLIP76 purified from transformed *E. coli* into proteoliposomes was done as described by us previously (28). Briefly,

purified RLIP76 was dialyzed against reconstitution buffer [10 mmol/L Tris-HCl (pH 7.4), 4 mmol/L MgCl₂, 1 mmol/L EGTA, 100 mmol/L KCl, 40 mmol/L sucrose, 2.8 mmol/L β-mercaptoethanol, 0.05 mmol/L butylated hydroxytoluene, and 0.025% polidocanol]. An aqueous emulsion of soybean asolectin (40 mg/mL) and cholesterol (10 mg/mL) was prepared in the reconstitution buffer by sonication, from which a 100 μL aliquot was added to 0.9 mL of dialyzed purified RLIP76 containing 20 μg of protein. After sonication of the resulting mixture for 30 seconds at 50 W, 200 mg of SM-2 Bio-beads pre-equilibrated with reconstitution buffer (without polidocanol) were added to initiate vesiculation, and after 4 hours of incubation at 4°C, SM-2 beads were removed by centrifugation at 3,620 × g. Control vesicles (control liposomes) were prepared using an equal amount of crude protein from *E. coli* not expressing RLIP76.

Transport Studies in rec-RLIP76 Proteoliposomes. ATP-dependent transport of ³H-vinorelbine in the rec-RLIP76 reconstituted proteoliposomes was carried out by the rapid filtration technique described by us previously (24). In a 100-μL reaction mixture, aliquots of proteoliposomes were mixed in the transport buffer. To this solution, ³H-vinorelbine (specific activity 4,150 cpm/pmol) was added to achieve a final concentration of 100 nmol/L, and the mixtures were allowed to equilibrate at 37°C for 5 minutes. The transport reaction was initiated by addition of buffer without or with 4 mmol/L ATP and incubated for 5 minutes at 37°C with gentle shaking. After the reaction was stopped by placing the tubes in ice, 30-μL aliquots of the mixture were filtered through nitrocellulose membrane (0.45 μm) into a 96-well filtration plate under uniform suction. The plate was then air-dried and the filters cut by Millipore punch-hole assembly. Filters were subsequently placed individually in glass scintillation vials containing 10 mL of scintillation fluid. Radioactivity was determined in triplicate using a liquid scintillation counter. Net ATP-dependent transport of vinorelbine was determined by subtracting vesicular uptake in presence of NaCl from that measured in the presence of ATP, and the transport rate was calculated in terms of pmol per min per mg protein. The effect of RLIP76-mediated uptake of substrate by vesicles was studied by comparing uptake with or without ATP by liposomes prepared in the similar manner as described above, except without addition of RLIP76. The transport of ¹⁴C-doxorubicin (specific activity, 9.0 × 10⁴ cpm/nmol, use 3.6 μmol/L final concentration) was done in a similar manner.

Kinetics of ATP-Dependent Vinorelbine Transport. ATP-dependent vinorelbine transport kinetics were evaluated at seven vinorelbine concentrations between 20 and 200 nmol/L with ATP concentration fixed at 4 mmol/L to obtain the K_m for vinorelbine and at six ATP concentrations between 1 and 10 mmol/L with vinorelbine concentration fixed at 100 nmol/L to obtain the K_m for ATP. Triplicate measurements of uptake were done in the absence and presence of ATP in both control liposomes and proteoliposomes at each of the seven concentrations of vinorelbine and six concentrations of ATP, and double reciprocal plots of 1/v versus 1/[S] were generated to determine K_m. To determine whether doxorubicin was an inhibitor of vinorelbine transport or vinorelbine was an inhibitor of doxorubicin transport, we measured ATP-dependent vinorelbine uptake in the presence of seven concentrations of doxorubicin (0-10 μM) and doxorubicin uptake in the presence of nine concentrations of vinorelbine (0-10 μmol/L). Data were analyzed in Statistica using nonlinear regression.

Purification of RLIP76 from SCLC and NSCLC. DNP-SG affinity resin was prepared and used for purification of RLIP76 from membrane fraction of lung cancer cell lines as previously described (25).

Transfection of RLIP76 in SCLC and NSCLC Cells. H1618 (SCLC) and H358 (NSCLC) were transfected with the eukaryotic expression vector alone (pcDNA3.1) or with pcDNA3.1-RLIP76 using Effectene Transfection Reagent kit (Qiagen, Valencia, CA). Expression of RLIP76 mRNA in lung cancer cell lines was evaluated by reverse transcription-PCR analysis. The RNA was prepared by RNeasy kit (Qiagen). RNA was quantified and purity was determined by measuring absorbance at 260 and 280 nm. RLIP76 gene-specific primers [334-353 bp (upstream primer) and 1,209-1,228 bp (downstream primer)] were used for reverse transcription-PCR. Ready-to-go reverse transcription-PCR beads were used according to the manufacturer's instructions (Amersham Biosciences, Piscataway, NJ). Levels of

RLIP76 protein in control and transfected clones were measured by immunoassay using anti-RLIP76 IgG. Aliquots of crude detergent membrane fraction of cells containing 100 μg protein were applied to SDS-PAGE, and Western blot analyses was done according to the method of Towbin et al. (37).

Inhibition of Vinorelbine Efflux from Lung Cancer Cells by Anti-RLIP76 IgG. Fixed number of cells were plated into each well of the microtiter plates as described above for drug sensitivity assays. After overnight incubation at 37°C, 37.5 $\mu\text{g}/\text{mL}$ anti-RLIP76 IgG antibodies (final concentration) were added to the cells and incubated for an additional 24 hours. Anti-RLIP76 antibodies used in these experiments were previously shown by Ouchterlony double immunodiffusion tests to be noncross-reactive with any other proteins including PgP or MRP-1 (25). Upon removal of the antibody and addition of fresh medium, vinorelbine aliquots were added and the resulting IC_{50} from the concomitant interaction between chemotherapeutic drug and antibody was determined in accordance with the aforementioned drug sensitivity procedure (27).

Chou-Talalay Median Effect Analysis of Synergy. The Calcusyn software package (Biosoft, Ferguson, MO) employing the Chou-Talalay method of determination of synergy was used to assess synergism, antagonism, and additive effects of interaction as described (39). Briefly, the analysis uses an algorithm that takes into account the cytotoxicity as well as dose-effect curves for vinorelbine and anti-RLIP76 IgG antibodies to generate a combination index. Combination index < 1 , 1 and > 1 correspond to synergy, additivity, and antagonism, where synergy indicates IC_{50} adjustment greater than the expected additive effect and antagonism indicates IC_{50} adjustment less than the expected additive effect.

Preparation of Membrane Inside-Out Vesicles from Cells. Crude membrane vesicles (inside-out vesicles, IOV) were prepared from the human lung cancer cell lines using established procedures as described by us for the human erythrocytes (24) and K562 cells (28).

Transport Studies in IOVs. Transport studies in IOVs were done by the same method as described above for the RLIP76-proteoliposomes, except that instead of the no-protein proteoliposome, we used heat-inactivated IOVs as negative controls.

^3H -Vinorelbine Uptake Studies. The NSCLC (H358) wild type, empty vector (pcDNA3.1), or RLIP76-pcDNA3.1 transfected cells were harvested washed with PBS and aliquots containing 5×10^6 cells (in triplicate, for each time point) were inoculated into fresh medium. After overnight incubation, the cells were pelleted and resuspended in 90 μL medium. [^3H]-Vinorelbine (100 nmol/L; specific activity, 4,150 cpm/pmol) was then added to the medium and incubated for 5, 10, 20, 30, and 60 minutes at 37°C. Drug uptake was stopped by rapid cooling on ice. Cells were centrifuged at $2,000 \times g$ for 5 minutes at 4°C and medium was completely decanted. Radioactivity was determined in the cell pellet after washing twice with ice-cold PBS.

^3H -Vinorelbine Efflux Studies. The NSCLC (H358) wild type, empty pcDNA3.1-vector or RLIP76-pcDNA3.1 transfected cells were harvested washed with PBS and aliquots containing 5×10^6 cells (in triplicate) were inoculated into fresh medium. After overnight incubation, the cells were pelleted and resuspended in 90 μL medium. ^3H -Vinorelbine (100 nmol/L; specific activity, 4,150 cpm/pmol) was then added to the medium and incubated for 60 minutes at 37°C. Cells were centrifuged at $300 \times g$ for 5 minutes, after which the supernatant was removed completely and the cell pellet washed with PBS twice. The pellet was immediately resuspended in 1 mL of PBS; 50 μL aliquots (clear supernatant) were removed every minute for radioactivity counting for 15 minutes. The back-added curves of cellular residual vinorelbine versus time were constructed as described previously (40).

Immunofluorescence and Confocal Laser Scanning Microscopy. For immunohistochemical localization of RLIP76, H358 NSCLC cells ($\sim 1 \times 10^6$ cells) were grown on sterilized glass coverslips in 12-well plates. After 24 hours, 10% goat serum was added for 60 minutes at room temperature to block nonspecific binding. Subsequently, anti-RLIP76 IgG was added at the concentration of 100 $\mu\text{g}/\text{mL}$ and incubated for 2 hours at room temperature in humidified chamber. After washing with PBS four to five times, FITC

conjugated secondary antibodies were added and incubated for 1 hour at room temperature in humidified chamber followed by washing with PBS four to five times. 4',6-Diamidino-2-phenylindole was used as a blue counterstain. Finally, coverslips were removed and dried in air and mounted on slides upside down with Vectashield mounting medium for fluorescence (Vector Laboratories). Pictures were taken using a Zeiss LSM 510META (Jena, Germany) laser scanning fluorescence microscope.

Results

Cell Surface Distribution of RLIP76. Confocal laser micrographs of live unfixed H358 NSCLC cells examined for cell surface expression by immunohistochemistry showed cell surface recognition by anti-RLIP76 polyclonal IgG (Fig. 1A). Under these conditions, no cell surface signal was detected when the preimmune serum IgG was used as the primary antibody. Deletion mutant analyses of the NH_2 -terminal of RLIP76 have confirmed that residues 171 to 185 comprise a cell surface domain (41).

Cytotoxicity of Vinorelbine and Doxorubicin. Although doxorubicin has some activity, clinically vinorelbine is significantly superior in NSCLC, highlighted by recent finding of improved survival with vinorelbine chemotherapy in NSCLC (5). This difference in efficacy is also evident in cytotoxicity assays in cultured lung cancer cell lines (Table 1). It is interesting to note that the IC_{50} for doxorubicin is in the range of the K_m of doxorubicin for transport by RLIP76 ($\sim 3 \mu\text{mol}/\text{L}$), so that the activity of RLIP76 could be expected to affect doxorubicin sensitivity, as our previous results indicate (25, 28). The IC_{50} values for vinorelbine were two orders of magnitude lower than the K_m values for other xenobiotics transported by RLIP76 (micromolar range). Present studies were undertaken to determine whether vinorelbine was a transport substrate for RLIP76, whether RLIP76 would confer an accumulation defect and resistance to vinorelbine, and to explore the relationship between time of drug exposure, drug sensitivity and kinetic variables of drug transport.

Functional Reconstitution of RLIP76 in Liposomes. To determine whether vinorelbine is transported by RLIP76, we first studied the transport of radiolabeled vinorelbine in the differential response of NSCLC to vinorelbine; we proceeded to directly show transport by reconstituting purified RLIP76 into artificial proteoliposomes as described by us previously (28). For these experiments, RLIP76 was purified from transformed *E. coli* BL21(DE3) expressing recombinant RLIP76. Purity of RLIP76 used for reconstitution in proteoliposomes was assessed by SDS-PAGE and Western blot against anti-RLIP76 IgG (Fig. 1B and C). In SDS-PAGE, RLIP76 showed characteristic bands near 95 and 38 kDa, with a pattern of minor bands near 67 and 49 kDa. These bands arise from proteolytic degradation, and NH_2 -terminal sequencing of these bands reveal internal sequences of RLIP76 (28, 29). Amino acid composition analysis of total protein revealed that the amino acid content was within 96% of expected yields computed on the basis of the derived sequence of RLIP76. These findings rule out significant contamination with ABC transporters. Artificial proteoliposomes were prepared in the presence of 20 $\mu\text{g}/\text{mL}$ purified RLIP76, and control proteoliposomes were prepared in the presence of 20 $\mu\text{g}/\text{mL}$ crude membrane protein from *E. coli* used for purification of RLIP76. These proteoliposomes were stringently characterized for their size and sidedness to establish their suitability for transport studies as described by us (28). Uptake was quantified by rapid filtration 5 minutes after the addition of buffer without or with 4 mmol/L ATP to proteoliposomes. Results of vinorelbine uptake in the absence or presence of ATP in rec-

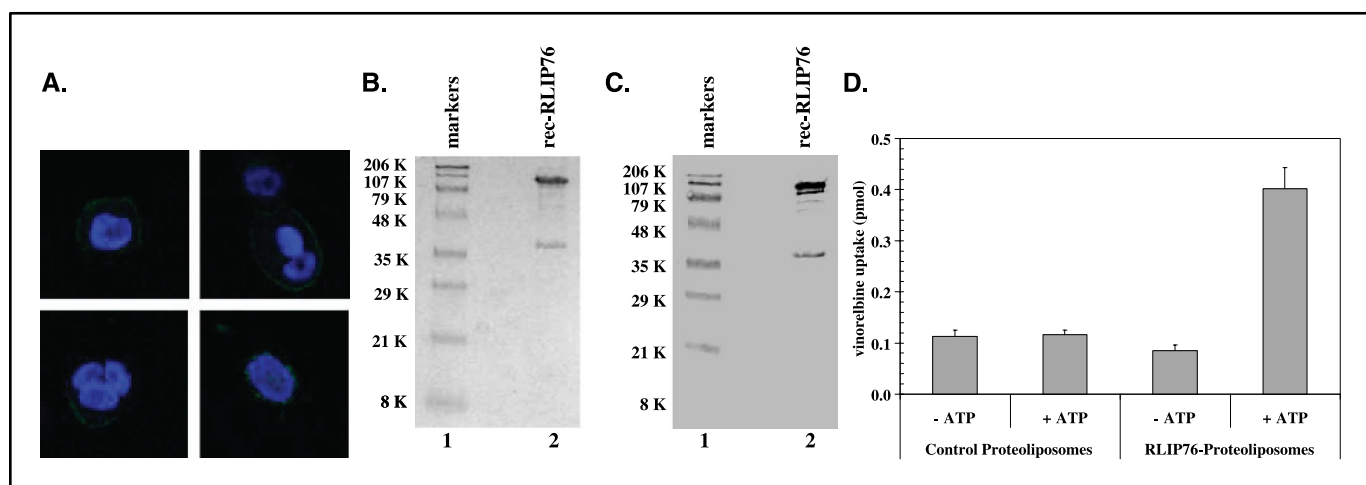


Figure 1. Expression of RLIP76 on the cell surface in H358 NSCLC and purification of rec-human RLIP76. For cell surface localization of RLIP76 in H358 NSCLC (A), cells were grown on glass coverslips and live, unfixed cells were subjected to immunohistochemistry using anti-RLIP76 IgG as primary antibody, and FITC-conjugated goat anti-rabbit IgG as secondary antibody. 4',6-Diamidino-2-phenylindole was used as a nuclear counterstain. Slides were analyzed using a Zeiss LSM 510META laser scanning fluorescence microscope. SDS-PAGE (B) and Western blot analyses (C) of RLIP76 expressed in *E. coli* BL21(DE3) transformed with full length RLIP76 cDNA, and purified as described in Materials and Methods. Purified enzyme was subjected to SDS-PAGE and Western Blot analyses. SDS-PAGE was stained with Coomassie brilliant blue R-250 and Western blots were done using anti-RLIP76 IgG as primary antibody and horseradish peroxidase-conjugated goat anti-rabbit IgG as secondary antibody and developed with 4-chloro-1-naphthol as chromogenic substrate. The uptake of radiolabeled vinorelbine by control- or RLIP76-proteoliposomes (D) was compared in the presence or absence of ATP. The proteoliposomes were incubated at 37°C with vinorelbine (100 nmol/L) for 5 minutes before addition of buffer without or with ATP, and uptake was measured 5 minutes after ATP addition. Filtered aliquots (30 μ L) contained 62.5 μ g lipid (4:1, asolectin/cholesterol) and 0.25 μ g protein (either RLIP76 or crude *E. coli* protein). Total radioactivity retained by 0.45- μ m filters in 96-well plates was determined after solubilizing filters, converted to pmol using the specific activity of vinorelbine (4,150 cpm/pmol). Column, average calculated from 12 measurements (control- or RLIP-proteoliposomes, without or with ATP, in triplicate); bar, SD. Uptake in RLIP76-liposomes with ATP is significantly greater than other groups ($P < 0.001$).

RLIP76 and control liposomes (Fig. 1D) showed significantly greater vinorelbine uptake in the presence of ATP, but only when recombinant RLIP76 was present ($P < 0.0001$). ATP did not affect vinorelbine uptake in control liposomes. ATP-dependent vinorelbine uptake by RLIP76-proteoliposomes was found to be temperature dependent, with an optimal activity near 37°C, and loss of activity at higher temperature (Fig. 2A). ATP-dependent transport decreased inversely with respect to extravesicular osmolarity (Fig. 2B), indicating that the majority of ATP-dependent uptake of vinorelbine by RLIP76-proteoliposomes was due to increased intravesicular accumulation, due to transmembrane movement of vinorelbine. Extrapolation to zero intravesicular volume (at infinite extravesicular sucrose concentration) to quantify the membrane bound fraction of vinorelbine indicated that very little vinorelbine was bound to the vesicle membrane. Compartment analysis of uptake with respect to time indicated a single compartment model of uptake ($\tau = 3.6 \text{ min}^{-1}$; Fig. 2C). When proteoliposomes were reconstituted with varying amounts of protein (between 5 and 50 μ g/mL) and equal amounts of vesicles were used for uptake studies, the uptake was found to be linear with respect to protein, indicating that transport rate was clearly determined by the amount of RLIP76 used for assay (Fig. 2D). Kinetics of transport were studied with respect to ATP and vinorelbine (Fig. 3A and B, respectively) and showed saturable kinetics consistent with an enzyme catalyzed activity, with K_m for ATP of 3.3 mmol/L, and K_m for vinorelbine of 75 nmol/L. Although ATP kinetics obeyed hyperbolic kinetics, vinorelbine kinetics was sigmoid with a Hill coefficient of 2, indicating cooperativity. We have observed similar behavior for colchicine transport (32). These findings suggest two binding sites for vinorelbine, perhaps as a result of RLIP76 dimer formation, perhaps through interactions at the leucine-zipper domain. Our

earlier studies indicated that the COOH-terminal of RLIP76 could form RLIP76 homodimers (29). Vinorelbine transport was inhibited by doxorubicin, and doxorubicin transport by vinorelbine (Fig. 3C and D). Taken together, our results show that vinorelbine is a substrate (allocrite) for ATP-dependent transmembrane transport by RLIP76.

RLIP76 Confers Vinorelbine Resistance in H358 NSCLC.

Because RLIP76 functions as an active transporter of vinorelbine in artificial liposomes, we studied RLIP76-catalyzed efflux of vinorelbine in NSCLC and SCLC. Furthermore, we reasoned that cells overexpressing RLIP76 would display a vinorelbine accumulation defect and enhanced vinorelbine resistance. Two RLIP76-expressing sublines of H-358 NSCLC and H-1618 SCLC were obtained after transfection with RLIP76. No vinorelbine or doxorubicin drug selection was used. Results of SDS-PAGE and Western blot analysis indicated that the RLIP76 overexpressing cells contained modestly increased RLIP76 protein (~2.5- to 3-fold) compared with the wild-type or vector-alone transfected lines (Fig. 4A and B).

The IC_{50} for vinorelbine and doxorubicin were measured with 12 or 96 hours of drug exposure time. Resistance to both doxorubicin and vinorelbine was clearly apparent in the RLIP76 overexpressing SCLC (Fig. 5A and B) as well as NSCLC cell line (Fig. 5C and D), although the degree of resistance was much greater in the 12-hour assay, where the concentrations of vinorelbine were an order of magnitude higher than that used in the 96-hour assay. Please note the differences in scales between the panels in Fig. 5. We have previously shown anti-RLIP76 antibodies recognize a cell surface epitope of RLIP76 and inhibit its transport activity for doxorubicin, thus synergistically enhance doxorubicin cytotoxicity through increased intracellular accumulation of doxorubicin (27). We have also shown through titration studies (26) that anti-RLIP76 at 37.5 μ g/mL is sufficient to fully

block RLIP76 under present conditions. When this concentration of anti-RLIP76 IgG was included in the cytotoxicity assay done at both 12 and 96 hours duration of drug exposure, increased cytotoxicity of vinorelbine was apparent at the 12 hours (high dose) as well as the 96 hours (low dose) exposure, but was clearly more prominent in the 12-hour (high dose) exposure study. The effect of anti-RLIP76 IgG and vinorelbine in the 12-hour assay was clearly synergistic, with combination index of 0.3 in Chou-Talalay analysis of synergy. Taken together, these results show for the first time that transfection with RLIP76 confers resistance to vinorelbine. Abrogation of this resistance by specific anti-RLIP76 antibodies further indicates that this effect is specifically mediated by RLIP76.

Effect of RLIP76 Overexpression on Accumulation and Efflux of Vinorelbine in Cells. To determine whether the acquired resistance of transfected cells was due to enhanced RLIP76-mediated efflux and consequently diminished accumulation, we conducted drug uptake and efflux studies with wild-type and RLIP76 transfected intact H358 cells. For uptake studies, cellular vinorelbine accumulation was quantified at varying times after addition of drug to the extracellular medium (Fig. 6A). The total vinorelbine accumulation was markedly reduced in RLIP76 overexpressing cells. These results were consistent with increased transport of vinorelbine in RLIP76 overexpressing cells and were in agreement of the results of efflux studies described below. In

Table 1. Vinorelbine IC₅₀ values in NSCLC

Cell lines	IC ₅₀ (μmol/L)	
	Vinorelbine	doxorubicin
H358	0.06 ± 0.008	5.0 ± 0.6
H226	0.065 ± 0.008	6.5 ± 0.7
H520	0.08 ± 0.01	6.0 ± 0.6
H1395	0.05 ± 0.006	5.0 ± 0.4
H2126	0.045 ± 0.006	4.5 ± 0.5
H2347	0.08 ± 0.01	4.0 ± 0.3

NOTE: Drug sensitivity assays were performed using 3-(4,5-dimethylthiazol-2-yl)-2,5-diphenyltetrazolium bromide (at 12 hours) to determine IC₅₀ values. The values are presented as mean ± SD from three separate determinations with eight replicates each (*n* = 24).

experiments designed to measure the efflux of vinorelbine, we loaded cells with radiolabeled vinorelbine by incubating cells with the drug for 60 minutes, followed by rapid dilution in drug-free medium, and taking sequential aliquots of external medium for radioactivity. Cell-associated drug was calculated by back-addition as previously described (40) and plotted with respect to time. The rate of loss of vinorelbine from cells due to efflux was significantly greater for RLIP76 transfected H358 cells as compared with the wild-type or vector-alone transfected cells (Fig. 6B). Taken together, these findings show that in RLIP76-overexpressing cells drug accumulation is diminished due to increased efflux of vinorelbine as compared with the wild-type cells. These results further confirm that vinorelbine is a transport substrate for RLIP76.

Transport of Vinorelbine by IOVs Prepared from SCLC and NSCLC Membranes. To further confirm that RLIP76-mediated vinorelbine transport in these cells, we measured vinorelbine transport in crude membrane IOVs prepared from wild-type or vector or RLIP76 transfected H358 NSCLC and H1618 SCLC cell lines. Results of these studies showed that the ATP-dependent transport of vinorelbine was increased significantly (*P* < 0.01) in the IOVs prepared from RLIP76-transfected SCLC and NSCLC cell line (Fig. 6C and D). In our previous studies, we have shown that the transport rate of doxorubicin was greater in the wild-type NSCLC cell line as compared with the SCLC cell line (26), and the effect of RLIP76 overexpression was more prominent in the NSCLC as compared with SCLC cell line. Parallel results obtained on transport of vinorelbine by these cells strongly indicate that both doxorubicin and vinorelbine are transported by RLIP76, and the rate of efflux of these drugs correlates with the amount of RLIP76 expressed in these cells.

Discussion

Present studies show that RLIP76 is capable of mediating ATP-dependent efflux of vinorelbine in lung cancer cells, and that increased RLIP76 can confer resistance to vinorelbine in these cells by conferring an accumulation defect mediated by the efflux of drug from cells. Vinorelbine transport by RLIP76 was shown in an isolated system, which has been shown previously to be clearly devoid of MRP1 or Pgp. In this system, RLIP76 clearly is necessary and sufficient to mediate the *trans*-membrane, anti-gradient, ATP hydrolysis dependent, temperature-sensitive, and saturable transport of vinorelbine into artificial liposomes. These findings are

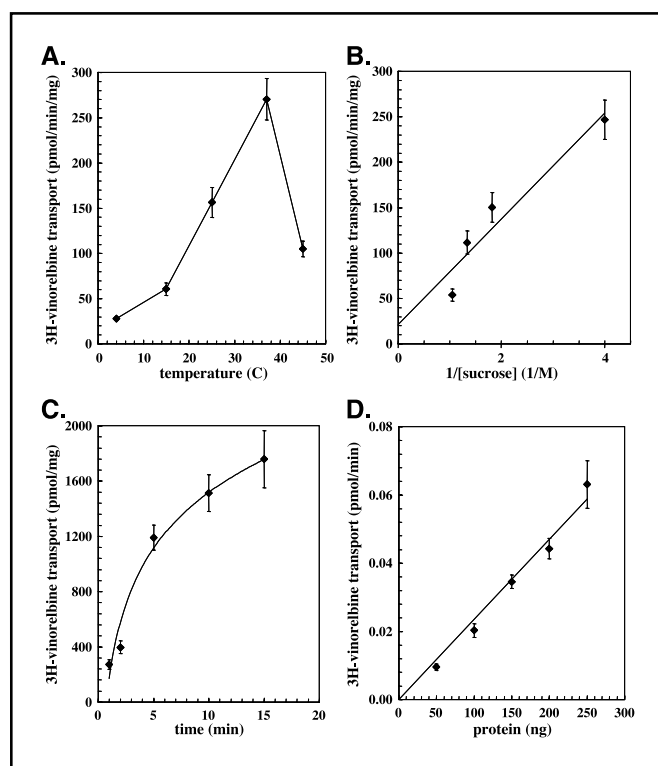


Figure 2. Characterizations of RLIP76-mediated vinorelbine transport. Transport studies were carried out as described in Methods. Points average calculated from 12 measurements (control- or RLIP-proteoliposomes, without or with ATP, in triplicate); bars, SD. One of the variables (temperature, extravesicular sucrose, time, and vesicle protein) was varied holding the other constant at standard conditions which include 100 nmol/L vinorelbine, 4 mmol/L ATP, 40 mmol/L extravesicular sucrose, 250 ng protein/30 μL aliquot filtered, temperature 37°C, and 5 minutes incubation after addition of ATP. Results shown are for temperature dependence (A), osmolar dependence (B), time dependence (C), and RLIP76-protein dependence (D).

strengthened by transport studies in membrane IOVs showing a proportional increase in vinorelbine transport in RLIP76 over-expressing cells and by intact cell studies showing that RLIP76 transfection confers decreased vinorelbine accumulation mediated by increased rate of efflux from intact cells. The resistance to vinorelbine conferred by RLIP76 overexpression and sensitization of vinorelbine by blocking RLIP76 is further evidence to support the assertion that RLIP76 can function as a vinorelbine transporter in these cells, and that it may contribute to vinorelbine resistance, particularly under conditions of high concentration and short duration exposure. The maximal velocity of vinorelbine transport 0.3 nmol per min per mg determined during the present studies was found to be significantly lower than reported previously for doxorubicin ~ 26 nmol per min per mg (26, 28). The K_m for transport for vinorelbine was also significantly lower, 75 nmol/L, as compared with 3 $\mu\text{mol/L}$ for doxorubicin. These findings suggest that RLIP76 is comparatively more efficient in the removal of doxorubicin through transport from lung cancer cells, as compared with vinorelbine. The greater impact of RLIP76 on vinorelbine resistance in the high dose/short time of exposure IC_{50} assay as

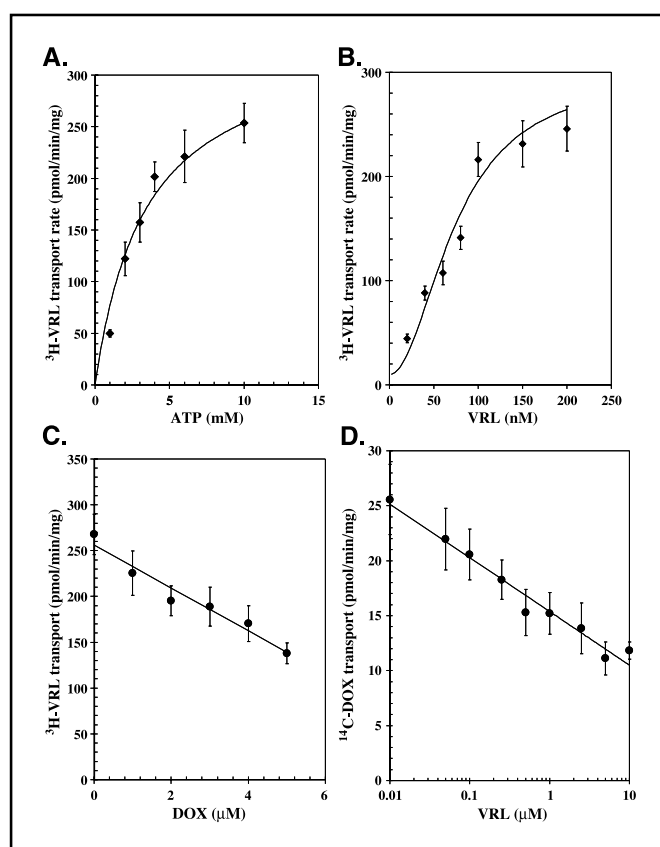


Figure 3. Kinetics of RLIP76-mediated vinorelbine transport and mutual inhibition of vinorelbine and doxorubicin transport. Transport under varying vinorelbine or ATP concentration. The kinetics for ATP was done with vinorelbine fixed at 100 nmol/L, and for vinorelbine kinetics, ATP was fixed at 4 mmol/L. Transport rates were plotted versus drug concentration and analyzed by nonlinear regression. Results for ATP kinetics are shown (A). For vinorelbine kinetics (B), the data were analyzed using the Hill equation. Points, average from triplicate determinations; bar, SD. The transport of vinorelbine (100 nmol/L) was studied in the presence of varying concentration of doxorubicin (C) and the transport of doxorubicin (3.6 $\mu\text{mol/L}$) was studied in the presence of varying concentration of vinorelbine (D). Point, average calculated from 12 measurements (control- or RLIP-proteoliposomes, without or with ATP, in triplicate); bar, SD.

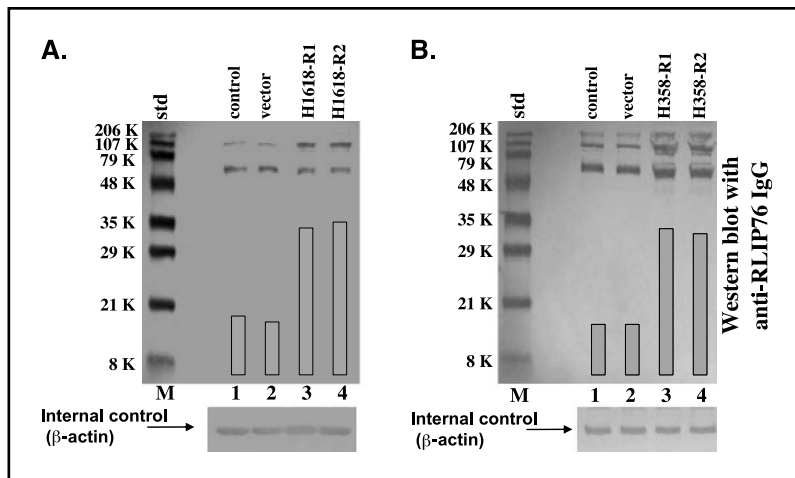
compared with the low-dose/long-time exposure is consistent with this assertion, because the K_m for vinorelbine transport is significantly greater than the IC_{50} for vinorelbine observed with the 96-hour exposure; on the other hand, higher drug concentration required to achieve IC_{50} in the 12-hour exposure studies are well within the range of the K_m for vinorelbine transport by RLIP76.

Although, rigorous proof is lacking for vinorelbine transport by ABC transporters in isolated systems with purified protein reconstituted into artificial liposomes, given their ability to transport other *Vinca* alkaloids, it is quite likely that these are also playing a role. Although in present transport studies done in crude membrane IOVs do not exclude a contribution of ABC transporters, the expression of MRP-1, MRP-3, and MRP-5 as well as Pgp has been examined in these cell lines and shown to be unaffected by RLIP76 overexpression.³ Thus, the observed increased vinorelbine transport rate is not due to a confounding effect of at least these transporters. In contrast, earlier drug transport studies with numerous ABC transporters have not specifically examined the potential confounding effects of differential RLIP76 expression and leave open the possibility that inconsistencies and lack of clinical correlations between ABC transporter expression and clinical drug resistance may be partially due to differential RLIP76 expression.

Our findings are of significance with respect to chemotherapy of lung cancer from several viewpoints. In addition to establishing, for the first time, that vinorelbine is a substrate for transport by RLIP76, these results put forth a novel kinetic and mechanistic explanation for the relative inefficacy of doxorubicin in lung cancer as compared with vinorelbine. Doxorubicin is a much better substrate for transport by RLIP76 as compared with vinorelbine thus would be more subject to RLIP76 mediated drug resistance. The rate of doxorubicin transport by RLIP76 is about 100-fold greater than that for vinorelbine. Furthermore, the IC_{50} for doxorubicin in NSCLC (~ 1 $\mu\text{mol/L}$) with 96 hours of exposure is well within the range of the K_m for doxorubicin transport by RLIP76, whereas the IC_{50} for vinorelbine, particularly in the 96 hours of exposure (~ 0.008 $\mu\text{mol/L}$) is well below the K_m for vinorelbine transport (0.075 $\mu\text{mol/L}$). These findings have potentially important consequences for administration of vinorelbine. Our findings also indicate that regimens of chemotherapy, which employ more frequent low-dose administrations or continuous infusions of vinorelbine, are likely to be more effective in bypassing drug resistance mediated by RLIP76. The lower peak concentrations of vinorelbine with repeated low-dose or continuous infusion regimens will not allow optimal transport by RLIP76. Perhaps most importantly, these findings offer a novel target for modulation of vinorelbine chemotherapy using small molecules, which could specifically bind to and inhibit transport activity of RLIP76. These findings suggest that nucleotide analogues such as those used as inhibitors of tyrosine or protein kinases as well as G-proteins could function as well through inhibition of transport activity of RLIP76. Indeed, our unpublished studies indicate specific binding and inhibition of the ATPase activity of RLIP76 by nucleotide analogues, as well as by kinase inhibitors such as genistein and calphostin-C. Because both ATPase domains of RLIP76 differ from the nucleotide-binding sites of ABC transporters and G-proteins, it may be possible to design relatively more specific inhibitors for RLIP76. However, the X-ray crystallographic structure

³ Awasthi et al., unpublished observations.

Figure 4. RLIP76 overexpression in H1618 and H358. Aliquots of crude detergent membrane fraction of cells from H1618 or H358 wild-type control, vector-alone transfected, or two RLIP76 transfected clones (*R1* and *R2*), containing 100 µg protein were applied in Western blot analyses against anti-RLIP76 IgG. Results were quantified by scanning densitometry of the full-length RLIP76 protein band near 109 kDa. β-actin was used as internal control.



of the nucleotide binding domains of RLIP76 will ultimately be necessary to design more specific inhibitors.

We believe these studies are of critical importance in understanding the role of transport-mediated resistance to vinorelbine in lung cancer, particularly because vinorelbine has proven to be one of the most effective drugs for NSCLC. Perhaps, the efficacy of vinorelbine and cisplatin combination is rooted in the fact that cisplatin is metabolized to glutathione conjugates.

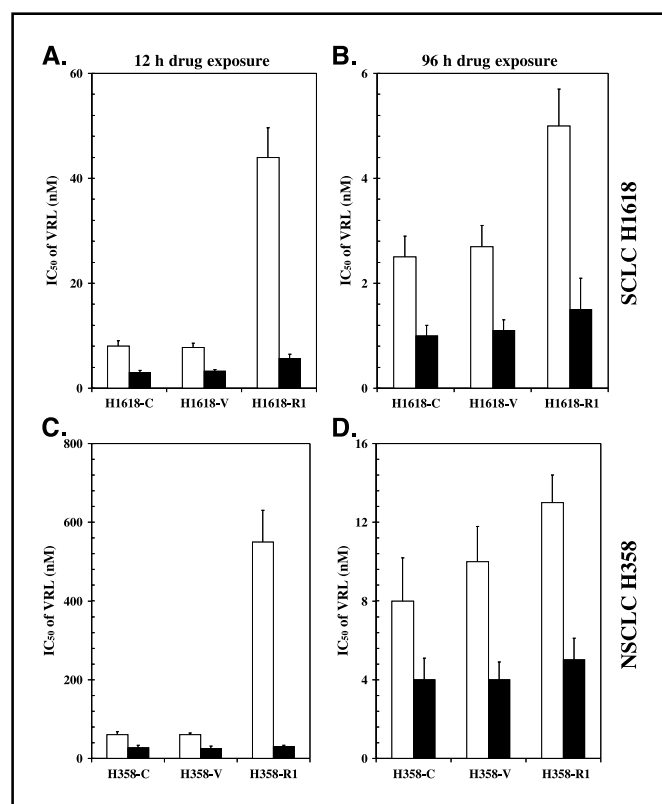


Figure 5. Effect of RLIP76 transfection, drug exposure duration, and anti-RLIP76 IgG on vinorelbine cytotoxicity in SCLC and NSCLC. MTT cytotoxicity assays were done by exposing cells to varying concentrations of vinorelbine for 12 or 96 hours in the presence of anti-RLIP76 IgG (37 µg/mL; filled columns) or an equal concentration of pre-immune IgG (open columns). Columns, average from two separate experiments, each with eight replicate values and 10 drug concentrations ranging from 1 to 10,000 nmol/L; bars, SD. Please note the differences in scales between panels.

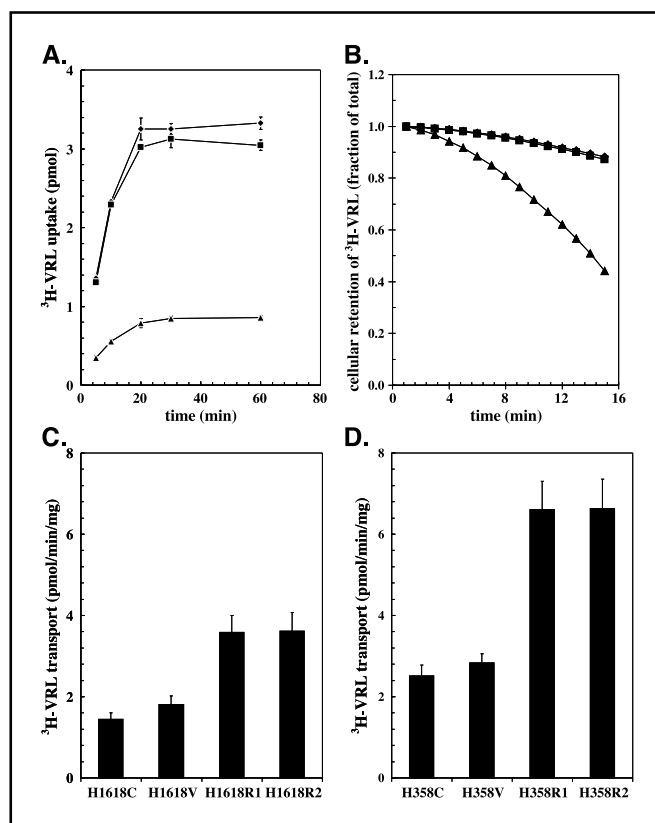


Figure 6. Effect of RLIP76 transfection on cellular vinorelbine accumulation and efflux from intact cells, and on vinorelbine transport by crude membrane IOVs from SCLC and NSCLC cells. The cellular accumulation of vinorelbine was determined by incubating washed H358 wild-type (♦), vector-alone transfected (■), and RLIP76-transfected (▲) cells with 100 nmol/L radiolabeled vinorelbine for varying time periods before washing off extracellular drug and determining cell-associated radioactivity (A). For intact cell efflux studies (B), attached cells were loaded with vinorelbine by incubating for 60 minutes in the presence of 100 nmol/L vinorelbine, followed by rapid dilution in drug-free buffer. Aliquots of buffer were removed at 60-second intervals. The back-added curves of cellular residual vinorelbine versus time were constructed as described previously (40). Vinorelbine transport in IOVs prepared from crude membrane fraction of SCLC H1618 (C) and NSCLC H358 (D) cells were prepared and enriched for the IOV fraction using wheat-germ agglutinin affinity chromatography as described by us previously (24). Uptake of vinorelbine was determined in the absence or presence of 4 mmol/L ATP, and ATP-independent uptake was subtracted to obtain ATP-dependent uptake. Vinorelbine concentration was held constant at 100 nmol/L. Uptake was carried out for 10 minutes after addition of ATP. All studies were done at 37°C. Results from two experiments, each in triplicate (n = 6).

RLIP76 is known to transport glutathione conjugates of a number of electrophilic chemotherapeutic agents, and competitive inhibition by glutathione conjugates of transport of other natural product drugs has been shown for RLIP76. Studies to address the specific postulate that synergy between cisplatin and vinorelbine is contributed to by competitive inhibition of vinorelbine transport by cisplatin-glutathione conjugates are presently being carried out.

Acknowledgments

Received 8/9/2004; revised 10/26/2004; accepted 11/22/2004.

Grant support: USPHS grants CA 77495, CA104661 (S. Awasthi), and ES 012171 (Y.C. Awasthi).

The costs of publication of this article were defrayed in part by the payment of page charges. This article must therefore be hereby marked advertisement in accordance with 18 U.S.C. Section 1734 solely to indicate this fact.

We thank Dr. Nancy Rowe (Office of Information Technology, University of Texas at Arlington, Arlington, TX) for her assistance in the statistical analyses of the data.

References

- Nishio K, Nakamura T, Koh Y, Suzuki Y, Fukumoto H, Saijo N. Drug resistance in lung cancer. *Curr Opin Oncol* 1999;11:109-15.
- Gottesman MM, Fojo T, Bates SE. Multidrug resistance in cancer: role of ATP-dependent transporters. *Nat Rev Cancer* 2002;2:48-58.
- Giaccone G. The clinical significance of drug resistance in lung cancer. *Lung Cancer* 1997;18:S121.
- Cole SPC, Deeley RG. Biology of MRP in drug resistance of lung cancer. *Lung Cancer* 1997;18:S102-3.
- Einhorn L. Non-small cell lung cancer: improved chemotherapy. *Lung Cancer* 1997;18:111.
- Curran M, Plosker G. Vinorelbine A review of its use in elderly patients with advanced non-small cell lung cancer. *Drugs Aging* 2002;19:695-721.
- Cros S, Wright M, Morimoto M, Lataste H, Couzinier JP, Krikorian A. Experimental antitumor activity of Navelbine. *Semin Oncol* 1989;16:15-20.
- Gridelli C, Perrone F, Gallo C, et al. Chemotherapy for elderly patients with advanced non-small-cell lung cancer: the Multicenter Italian Lung Cancer in the Elderly Study (MILES) Phase III Randomized Trial. *J Natl Cancer Inst* 2003;95:362-72.
- Song SY, Kim WS, Kim K, et al. Vinorelbine, ifosfamide, and cisplatin combination as salvage chemotherapy in advanced non-small cell lung cancer. *Jpn J Clin Oncol* 2003;33:509-13.
- Mori K, Kamiyama Y, Kondo T, Kano Y, Tominaga K. Phase II study of the combination of vinorelbine and cisplatin in advanced non-small-cell lung cancer. *Cancer Chemother Pharmacol* 2004;53:129-32.
- Potier P. The synthesis of Navelbine prototype of a new series of vinblastine derivatives. *Semin Oncol* 1989;16:2-4.
- Ngan VK, Bellman K, Panda D, Hill BT, Jordan MA, Wilson L. Novel actions of the antitumor drugs vinflunine and vinorelbine on microtubules. *Cancer Res* 2000;60:5045-51.
- Toso C, Lindley C. Vinorelbine: a novel *Vinca* alkaloid. *Am J Health Syst Pharm* 1995;52:1287-304.
- Dumontet C, Branimir S. Mechanisms of action of and resistance to antitubulin agents: microtubule dynamics, drug transport, and cell death. *J Clin Oncol* 1999;17:1061-70.
- Stavrovskaya AA. Cellular mechanisms of multidrug resistance of tumor cells. *Biochemistry (Moscow)* 2000;65:95-106.
- Adams DJ, Knick VC. P-glycoprotein mediated resistance to 5'-nor-anhydro-vinblastine (Navelbine). *Invest New Drugs* 1995;13:13-21.
- Ueda K, Cardarelli C, Gottesman MM, et al. Expression of a full-length cDNA for the human "MDR1" gene confers resistance to colchicines, doxorubicin, and vinblastine. *Proc Natl Acad Sci U S A* 1997;84:3004-8.
- Cole SPC, Bhardwaj G, Gerlach JH, et al. Overexpression of a transporter gene in a multidrug-resistant human lung cancer cell line. *Science* 1992;258:1650-4.
- Debal V, Allam N, Morjani H, et al. Characterisation of a vinorelbine-resistant bladder carcinoma cell line cross-resistant to taxoids. *Br J Cancer* 1994;70:1118-25.
- Giaccone G, van Ark-Otte J, Rubio GJ, et al. MRP is frequently expressed in human lung cancer cell lines, in non-small cell lung cancer and in normal lungs. *Int J Cancer* 1996;66:760-7.
- Etievant C, Barret J-M, Kruczynski A, et al. Vinflunine (20',20'-difluoro-3',4'-dihydrovinorelbine), a novel *Vinca* alkaloid, which participates in P-glycoprotein (Pgp)-mediated multidrug resistance *in vivo* and *in vitro*. *Invest New Drugs* 1998;16:3-17.
- Lage H. ABC-transporters: implications on drug resistance from microorganisms to human cancers. *Int J Antimicrob Agents* 2003;22:188-99.
- Liscovitch M, Lavie Y. Cancer multidrug resistance: a review of recent discovery research. *IDrugs* 2004;7:388-9.
- Awasthi S, Singhal SS, Srivastava SK, et al. Adenosine triphosphate-dependent transport of doxorubicin, daunomycin, and vinblastine in human tissues by a mechanism distinct from the P-glycoprotein. *J Clin Invest* 1994;93:958-65.
- Singhal SS, Singhal J, Sharma R, et al. Role of RLIP76 in lung cancer doxorubicin resistance. I. The ATPase activity of RLIP76 correlates with doxorubicin and 4-hydroxynonenal resistance in lung cancer cells. *Int J Oncol* 2003;22:365-75.
- Awasthi S, Singhal SS, Singhal J, Cheng J, Zimniak P, Awasthi YC. Role of RLIP76 in lung cancer doxorubicin resistance. II. Doxorubicin transport in lung cancer by RLIP76. *Int J Oncol* 2003;22:713-20.
- Awasthi S, Singhal SS, Singhal J, Yang Y, Zimniak P, Awasthi YC. Role of RLIP76 in lung cancer doxorubicin resistance. III. Anti-RLIP76 antibodies trigger apoptosis in lung cancer cells and synergistically increase doxorubicin cytotoxicity. *Int J Oncol* 2003;22:721-32.
- Awasthi S, Cheng J, Singhal SS, et al. Novel function of human RLIP76: ATP-dependent transport of glutathione conjugates and doxorubicin. *Biochemistry* 2000;39:9327-34.
- Awasthi S, Cheng J, Singhal SS, et al. Functional reassembly of ATP-dependent xenobiotic transport by the N- and C-terminal domains of RLIP76 and identification of ATP binding sequences. *Biochemistry* 2001;40:4159-68.
- Cheng J, Sharma R, Yang Y, et al. Accelerated metabolism and exclusion of 4-hydroxynonenal through induction of RLIP76 and hGST5.8 is an early adaptive response of cells to heat and oxidative stress. *J Biol Chem* 2001;276:41213-23.
- Yang Y, Sharma A, Sharma R, et al. Cells preconditioned with mild, transient UVA irradiation acquire resistance to oxidative stress and UVA-induced apoptosis: role of 4-hydroxynonenal in UVA mediated signaling for apoptosis. *J Biol Chem* 2003;278:41380-8.
- Awasthi S, Singhal SS, Pandya U, et al. ATP-dependent colchicine transport by human erythrocyte glutathione conjugate transporter. *Toxicol Appl Pharmacol* 1999;155:215-26.
- Awasthi S, Singhal SS, He NG, et al. Modulation of doxorubicin cytotoxicity by ethacrynic acid. *Int J Cancer* 1996;68:333-9.
- Awasthi YC, Garg HS, Dao DD, Partridge CA, Srivastava SK. Enzymatic conjugation of erythrocyte glutathione with 1-chloro-2,4-dinitrobenzene: the fate of glutathione conjugate in erythrocytes and the effect of glutathione depletion on hemoglobin. *Blood* 1981;58:733-8.
- Zhao T, Singhal SS, Piper JT, et al. The role of glutathione S-transferases hGSTA1-1 and hGSTA2-2 in protection against oxidative stress. *Arch Biochem Biophys* 1999;367:216-24.
- Minamide LS, Bamburg JR. A filter paper dye-binding assay for quantitative determination of protein without interference from reducing agents or detergents. *Anal Biochem* 1990;190:66-70.
- Towbin H, Staehelin T, Gordon J. Electrophoretic transfer of protein from polyacrylamide gels to nitrocellulose sheets: procedure and some applications. *Proc Natl Acad Sci U S A* 1979;76:4350-3.
- Laemmli UK. Cleavage of structural proteins during the assembly of the head of bacteriophage T4. *Nature* 1970;227:680-5.
- Chou TC, Motzer RJ, Tong Y, Bosl GJ. Computerized quantitation of synergism and antagonism of taxol, topotecan, and cisplatin against human teratocarcinoma cell growth: a rational approach to clinical protocol design. *J Natl Cancer Inst* 1994;86:1517-24.
- Lin JT, Sharma R, Grady JJ, Awasthi S. A flow cell assay for evaluation of whole cell drug efflux kinetics: analysis of paclitaxel efflux in CCRF-CEM leukemia cells over-expressing p-glycoprotein. *Drug Metab Disp* 2001;29:103-10.
- Yadav S, Singhal SS, Singhal J, et al. Identification of Membrane Anchoring Domains of RLIP76 using Deletion Mutants Analyses. *Biochemistry*. In press 2005.